Estimation of Membrane Surface Potential and Charge Density from the Phase Equilibrium of a Paramagnetic Amphiphile†

J. David Castle‡ and Wayne L. Hubbell§,*

ABSTRACT: The distribution of a paramagnetic amphiphile, *N,N*-dimethyl-*N*-nonyl-*N*-tempoylammonium ion, between the membranes of charged phospholipid vesicles and the surrounding aqueous medium was studied by electron paramagnetic resonance spectroscopy. By systematically varying the surface charge of the vesicles and the aqueous electrolyte concentration, the distribution was shown to indicate vesicle surface potential. At each fixed phospholipid composition, the surface potential exhibited a dependence on aqueous NaCl concentration very similar to that predicted by the Gouy equation. The ability to sense and quantitate surface potentials makes this facile and sensitive technique of value in the study of cell and organelle surfaces.

At the interface between two nonmiscible phases, one aqueous and the other nonpolar, the existence of immobilized net charge gives rise to an electric field extending from the surface. If the mobile counterions and other ionic species present in the aqueous phase are assumed to be in thermal equilibrium, the presence of a field will cause their nonuniform distribution such that the ionic concentration at any point in the field will be described by the Boltzmann distribution $c = c_b \exp(-Ze\psi/kT)$, where c_b is the concentration in bulk solution remote from the field and c and ψ are, respectively, the concentration of the ion and the potential at the point in question (relative to a zero potential reference); Z,e,k,T are the ionic valence, electronic charge, Boltzmann constant, and absolute temperature, respectively.

Biological membranes constitute a thin nonpolar phase immiscible with aqueous phases on either side, and the constituent phospholipid and protein molecules give rise to a net charge on each of the interfaces. Studies of phospholipid (Rouser et al., 1968) and protein composition (Rosenberg and Guidotti, 1969) of the membrane have indicated that the net charge contributed by both classes of molecules is, in most cases, negative at physiologic pH. The resulting surface potential is clearly an important parameter in characterizing cell and organelle surfaces, and may be involved in regulating the interactions between membranes. In order to assess this latter possibility, and to investigate the capacities of particular cations to reduce the surface charge by specific binding, a simple and rapid method of estimating surface potentials is desirable.

Estimates of surface potentials for bilayer membranes have been obtained through the measurement of electrophoretic mobilities of cells and organelles. Studies of this type have been carried out on phospholipid liposomes (Barton, 1968; Haydon and Myers, 1973; McLaughlin and Harary, 1976), mitochondria (Thompson and McLees, 1961), adrenal chromaffin granules (Banks, 1966), and red blood cells (Haydon and Seaman, 1967; Seaman and Uhlenbruck, 1963). A second general approach taken to estimate surface potentials is based on the partition of charged indicator molecules between the aqueous medium and membrane surface. This method has been applied to proteins (Moller and Kragh-Hansen, 1975), detergent micelles (Moller and Kragh-Hansen, 1975), lipid monolayers (Haynes, 1974), and liposomes (Montal and Gitler, 1973). Finally, surface potentials have been estimated from the conductance of black lipid membranes doped with ion-selective carriers (McLaughlin et al., 1970, 1971; Muller and Finkelstein, 1972a,b; McLaughlin and Harary, 1976).

In this report, we describe a technique of the partition variety to estimate membrane surface potentials. Electron paramagnetic resonance (EPR[1]) is used to follow the distribution of the spin-labeled amphiphile, *N,N*-dimethyl-*N*-nonyl-*N*-tempoylammonium bromide (spin-label 1) between the

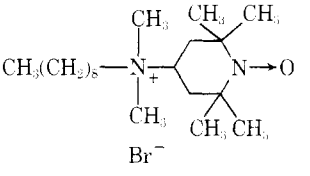

spin-label 1

membrane phase of sonicated phospholipid vesicles (containing phosphatidylcholine (PC) and phosphatidic acid (PA)) and the aqueous medium as a function of surface charge density. When associated with the membrane, this molecule exhibits a restricted mobility such that the spectral lines of its EPR signal are broadened relative to the lines for amphiphile free in solution. Consequently, it is possible to quantitate the amount of spin-labeled molecule present in each environment. The technique is of sufficient sensitivity that the cationic quaternary ammonium probe can be applied at levels low enough that it does not substantially affect the intrinsic charge of the electrostatic surface being tested. With this method, we

† From the Department of Chemistry, University of California, Berkeley, California 94720. *Received May 7, 1976.* This investigation was supported by National Institutes of Health Grant EY00729, the Alfred P. Sloan Foundation, The Camille and Henry Dreyfus Foundation, and the duPont Science Grant to Chemistry.

‡ Postdoctoral fellow of the Jane Coffin Childs Memorial Fund for Medical Research.

§ Alfred P. Sloan Foundation Fellow and Dreyfus Foundation Scholar.

[1] Abbreviations used are: EPR, electron paramagnetic resonance; PC, phosphatidylcholine; PA, phosphatidic acid; TLC, thin-layer chromatography; DCF, 2′,7′-dichlorofluorescein; DEAE-cellulose, diethylaminoethylcellulose; EGTA, ethylene glycol bis(β-aminoethyl ether)-*N,N*′-tetraacetic acid; GLC, gas-liquid chromatography; ANS⁻, 8-anilino-1-naphthalenesulfonate.

demonstrate that: (1) relative distribution coefficients for the spin-labeled amphiphile between phospholipid vesicles and the surrounding medium are readily estimated directly from first derivative spectra; (2) surface potentials of vesicles, as a function of surface charge (phospholipid composition) and aqueous salt concentration, can be calculated from the phase distribution data, the zero potential reference being chosen as vesicles formed entirely of PC; (3) the dependence of the experimentally determined surface potentials on salt concentration is in close agreement with that predicted by the Gouy equation at an estimated surface charge density based on the phospholipid composition of the vesicle.

Materials and Methods

Synthesis of the Paramagnetic Amphiphile. The spin-labeled amphiphile *N,N*-dimethyl-*N*-nonyl-*N*-tempoylammonium bromide was synthesized by one of us (W.L.H.) from *N,N*-dimethyl-4-amino-2,2,6,6-tetramethylpiperidine and *n*-nonyl bromide (in place of *n*-dodecyl bromide) as described previously (Hubbell et al., 1970). Following ion-exchange chromatography on AG 2-X8 anion-exchange resin in the bromide form, the compound was further purified by preparative thin-layer chromatography (TLC) on silica gel G (EM Laboratories, Elmsford, N.Y.). The nitroxide-containing amphiphile was dissolved and applied in methanol, and the plate was developed in chloroform–methanol–acetic acid–water 50:25:8:4. The nitroxide-containing molecule, easily located by its orange color, was scraped from the plate, dissolved in $CHCl_3$, concentrated by rotary evaporation, and dried. Its purity was tested by TLC in the above solvent system and was found to give a negative reaction with ninhydrin, a single spot when sprayed with Dragendorff's reagent and a single spot when sprayed with 0.1% 2′,7′-dichlorofluorescein (Stahl, 1969). The dried residue was then used directly for preparing stock solutions for EPR spectroscopy.

Preparation of Phosphatidylcholine. Phosphatidylcholine was purified from fresh hen eggs obtained locally, according to the procedure of Singleton et al. (1965), except that aluminum oxide (neutral, activity grade 3 from Woelm) was substituted for aluminum oxide (Merck) for column chromatography of the crude phosphatides dissolved in chloroform (5% (w/v)). Quantitation of the final product by gravimetric analysis and inorganic phosphate assay on ashed aliquots, according to the procedure of Chen et al. (1956), gave identical results.

Partial Purification of Phospholipase D. Phospholipase D was purified from Savoy cabbage, purchased locally, through the stage of cold acetone precipitation, according to the procedure of Davidson and Long (1958). To remove the amber-green pigmented material still present in the acetone precipitate, this crude preparation of phospholipase D was buffered with 10 mM potassium phosphate, pH 6.5, and loaded (at 4 °C) onto a DEAE-cellulose column (0.9-cm diameter and containing 1.3 g of DEAE-cellulose washed with 10 mM potassium phosphate, pH 6.5) (Yang et al., 1967). The column was eluted with a continuous gradient of NaCl, 0–500 mM in 10 mM potassium phosphate, pH 6.5. Enzymatic activity was located by testing the degradative capacity (on the substrate phosphatidylcholine) of aliquots of the column effluent. The assay mixtures were analyzed by silica gel TLC on microscope slides acidified with HCl vapors and developed with chloroform–methanol–HCl (concentrated) 87:13:0.5. The contaminating pigment, having an absorbance maximum at 715 nm (but no substantial absorbance at 280 nm), eluted before phospholipase D, which itself eluted before a second enzyme which utilized either PC or PA as substrate to yield an unidentified product of distinct mobility from PA. Fractions containing phospholipase D were pooled and used directly for bulk enzymatic cleavage of PC without quantitation of the enzymatic activity.

Preparation of Phosphatidic Acid. PA was prepared by enzymatic degradation of egg PC with phospholipase D. The bulk enzymatic degradation was carried out according to the procedure of Walker and Wheeler (1975), except that the volumes of the reaction mixture were doubled and the substrate PC was increased to 90 μmol/reaction vessel. The reactions were carried out at room temperature under nitrogen. The progress of the reaction was followed by TLC of the ether phase on silica gel G microplates (Peifer, 1962) acidified with HCl vapor before spotting and developed in chloroform–methanol–HCl (concentrated) 87:13:0.5. The spots corresponding to substrate PC (R_f ~0.22) and product PA (R_f ~0.33–0.66) were located by the $K_2Cr_2O_7$–H_2SO_4 charring method (Stahl, 1969). The time for completion of the conversion varied but was always 4 h or less. Upon termination of the reaction, the reaction mixtures were extracted successively with 2 volumes of diethyl ether, 1 volume of diethyl ether, and 2 volumes of chloroform. The organic phases were taken to dryness in a nitrogen-purged rotary evaporator (run at room temperature with a vacuum pump). The aqueous phase was discarded, but the residual white precipitate from the $CHCl_3$–H_2O interface was suspended in 25 ml of chloroform–methanol 2:1 (v/v). The lower phase was collected and taken to dryness in the flask containing dried residue of the previous organic extracts. The residues were resuspended in 30 ml of chloroform–methanol 2:1. At this point, 4 μCi of $^{45}CaCl_2$ (New England Nuclear (1 μCi/ml)) was equilibrated with this resuspension, and the removal of calcium was followed during subsequent purification by liquid scintillation counting. (70 mM $CaCl_2$ was required in the enzymatic preparation of PA and the latter has a reported apparent association constant for Ca^{2+} of ~10^4 (Barton, 1968; Abramson et al., 1966).) Initial extraction of the PA-containing resuspension, 1:1 (v/v) with 0.05 M EGTA–0.1 M NaCl (pH 7.5) (Walker and Wheeler, 1975), resulted in removal of only 45% of the $^{45}Ca^{2+}$. All PA remained in the lower organic phase by TLC. The organic phase was taken to dryness in a nitrogen-purged rotary evaporator and redissolved in 12 ml of chloroform–methanol 2:1. The preparation was then extracted with 0.2 volume of 1 N HCl and the lower organic phase was subsequently washed and clarified by centrifugation five times with 0.2 volume of distilled H_2O until the pH of the aqueous wash reached 5.5. Between each wash the organic phase was adjusted to original volume with chloroform–methanol 2:1. The HCl extraction and subsequent washes effected removal of $^{45}Ca^{2+}$ to a level of 99.6% of the original radioactivity (100% of the radioactivity being accounted for at each step). The organic phase was taken to dryness by rotary evaporation and redissolved in 1.8 ml of chloroform–methanol 2:1, and the PA was subsequently purified by preparative silica gel G TLC on three 20 × 20 cm plates preacidified with HCl vapors. The plates were developed at 4 °C in chloroform–methanol–HCl 87:13:0.5.[2] After development, PA was located on the nitrogen-dried plates by spraying a thin center strip (0.5 cm) of each plate with 0.1% DCF. PA (R_f 0.5–0.8) was scraped from the plates (excluding the stained center strip) leaving behind DCF-positive contaminants with R_f 0.20, 0.26, and 0.92. The

[2] A similar TLC procedure has been used by Romijn et al. (1972) for the purification of PA.

TABLE I: Fatty Acid Composition of PC and PA.

Fatty Acid Chain Length: No. Double Bonds	PC (mol %)	PA (mol %)
16:0	32.7	32.0
16:1	2.5	2.4
18:0	13.4	12.3
18:1	32.1	33.2
18:2	16.1	16.6
20:4	3.4	3.4

purified PA was eluted from the silica gel in a fritted glass funnel with chloroform–methanol–HCl (concentrated) 87:13:0.3, concentrated from 50 to 10 ml on a rotary evaporator, and washed six times with 0.2 volume of H_2O (the volume of the lower organic phase being adjusted to 10 ml with chloroform–methanol 2:1 between each wash) until the pH of the aqueous phase was 5.5. The final preparation was devoid of detectable $^{45}Ca^{2+}$ and contained no detectable unlabeled Ca^{2+} (<0.03 mol/mol of PA) following preparative TLC as determined by atomic adsorption. The product gave a single spot by TLC in either chloroform–methanol–HCl, 87:13:0.5, or hexane–acetone–formic acid, 74:26:0.25 (Possmeyer et al., 1969). Inorganic phosphate assay on ashed samples (Chen et al., 1956) gave a yield of 55% of the initial PC substrate. PA was stored at −20 °C in the free acid form in chloroform–methanol 2:1.

Determination of the Fatty Acid Composition of PC and PA. To verify that the fatty acid composition of the phospholipids used to prepare vesicles was the same, aliquots of each phospholipid were subjected to transesterification to form methyl esters of the fatty acids and subsequent identification by gas-liquid chromatography (GLC).

Each phospholipid (1.5 mg), dissolved in 1 ml of methanol along with 0.15 mg of heptadecanoic acid (used as an internal standard), was reacted according to the procedure of Tinoco et al. (1967). Heptadecanoic acid (0.45 mg) was processed as a separate sample for eventual characterization of its position in the elution profile from the gas-liquid chromatograph and for calibration of weight equivalents of peak areas.

GLC was performed at 155 °C on 1-μl aliquots of ester mixtures (dissolved in 100 μl of 2,2,4-trimethylpentane) in a Varian Aerograph Series 2400 chromatograph equipped with a column having diethylene glycol succinate as solid support and a flame ionization detector. Methyl esters obtained from Sigma Chemical Co. and Nu-chek Prep, Inc. (St. Louis, Mo., and Elysian, Minn.) were used as standards. The recorded peaks for the experimental samples were integrated manually using a compensating polar planimeter (Keuffel & Esser, Co.). As shown in Table I, the fatty acid compositions for PC and PA are very nearly the same. Additionally, in conjunction with the phosphate determination, the fatty acid:phosphate molar ratio was found to be 1.90 for PC and 2.00 for PA, another indication of absence of gross contamination.

Using the fatty acid composition presented in Table I, average molecular weights for PC and PA were calculated to be 770 and 684, respectively.

Preparation of Phospholipid Vesicles. Aliquots of stock lipids, stored under nitrogen at −20 °C, were removed in quantity to give 50 mg/ml of the appropriate combination of PC and PA in the final vesicle preparation. The solvent was removed under a flow of nitrogen, and the lipids were taken to dryness in a vacuum desiccator. Potassium phosphate buffer (pH 7.4, 1 mM) was added (1 ml/50 mg of dried lipid) and the samples were cooled in an ice bath and subjected to sonication (Sonifier, Heat Systems-Ultrasonics, Inc., Plainview, N.Y.) under nitrogen for 12–18 min at 35 W (the longer times being used for preparations containing smaller amounts of PA). The sonicates were subjected to centrifugation for 20 min at 31 000g_{av}, yielding pellets of titanium dust (from the sonifier tip) and tiny amounts of poorly sonicated lipid. The pH of the supernatants was carefully adjusted to 7.0 using 2 N NaOH, the amount of NaOH added being noted for eventual use in calculations of ionic strength. The stock vesicle suspensions, prepared in this manner, were stored under nitrogen prior to their dilution for surface-potential estimates. Where vesicle preparations were stored overnight, a 3-min resonication was performed 60 min prior to use.

Morphology of Sonicated Phospholipid Vesicles. Samples of phospholipid vesicles were prepared for electron microscopy by two different procedures.

(*1*) *Negative Staining.* Small volumes of stock vesicle preparations in buffer were diluted 100-fold with water, and 0.1 ml of the diluted suspension (0.05 (w/v)) was mixed with 0.6 ml of water and 0.1 ml of 4% osmium tetroxide. Fixation was carried out for 30 min at 0 °C. Drops of fixed vesicles were applied to formvar- and carbon-coated 200-mesh copper grids and, after 3 min, were negatively stained with 1% uranyl acetate.

(*2*) *Platinum Shadowing.* Small volumes of stock vesicle preparations were diluted 1000-fold with water. The diluted vesicles (~0.005% (w/v)) were fixed exactly as described above. Formvar- and carbon-coated 200-mesh copper grids were given a strongly positively charged surface by applying a drop of polylysine (10 mg/ml in H_2O, pH 7, mol wt_{av} = 3000, Sigma Chemical Co.). After 30 s, the grids were washed thoroughly with water (without drying) and then coated with a drop of the fixed vesicle suspension. After 3 min, each grid was washed with water, and 0.5% uranyl acetate (in water) was applied as a light negative stain to form a supporting glass around the vesicles. The grids were then positioned in a Balzers 510 freeze-fracture apparatus and shadowed by evaporating a 10–15 Å layer of platinum onto their surface at an angle of 45°. The shadowed preparations were examined and photographed at a magnification of 45 000 in a Philips 201 electron microscope.

Sample Preparation for EPR Measurements. The magnitude of the surface potential is a function of the aqueous ionic concentration. Variations in surface potential for fixed concentrations of nitroxide-labeled amphiphile and phospholipid (of specified PA–PC composition) were achieved by varying the aqueous concentration of NaCl. Samples were prepared from stock phospholipid vesicles (4.76% (w/v) lipid), 0.25 mM stock spin-label I in 1 mM potassium phosphate, pH 7.4, and NaCl prepared in 1 mM potassium phosphate, pH 7.4 (to give 0–400 mM final concentration). The samples were mixed 1 h before conducting EPR measurements, which typically lasted 4 h. Spectra were always recorded in the order of descending magnitude of surface potential (i.e., lowest NaCl concentration first).

Samples of 250 μl were contained in a Varian quartz flat cell. The Varian Model V-4500 spectrometer was operated in the X-band frequency range at a klystron power of 10 mW. The external magnetic field was scanned through 100 G with a time span of 5 or 10 min. The recorder response time was 0.3 s.

Measurements Using a Dual Sample Cell. To test spectral additivity for membrane-associated and bulk-aqueous spin-label, and to choose the best spectral representation of the total

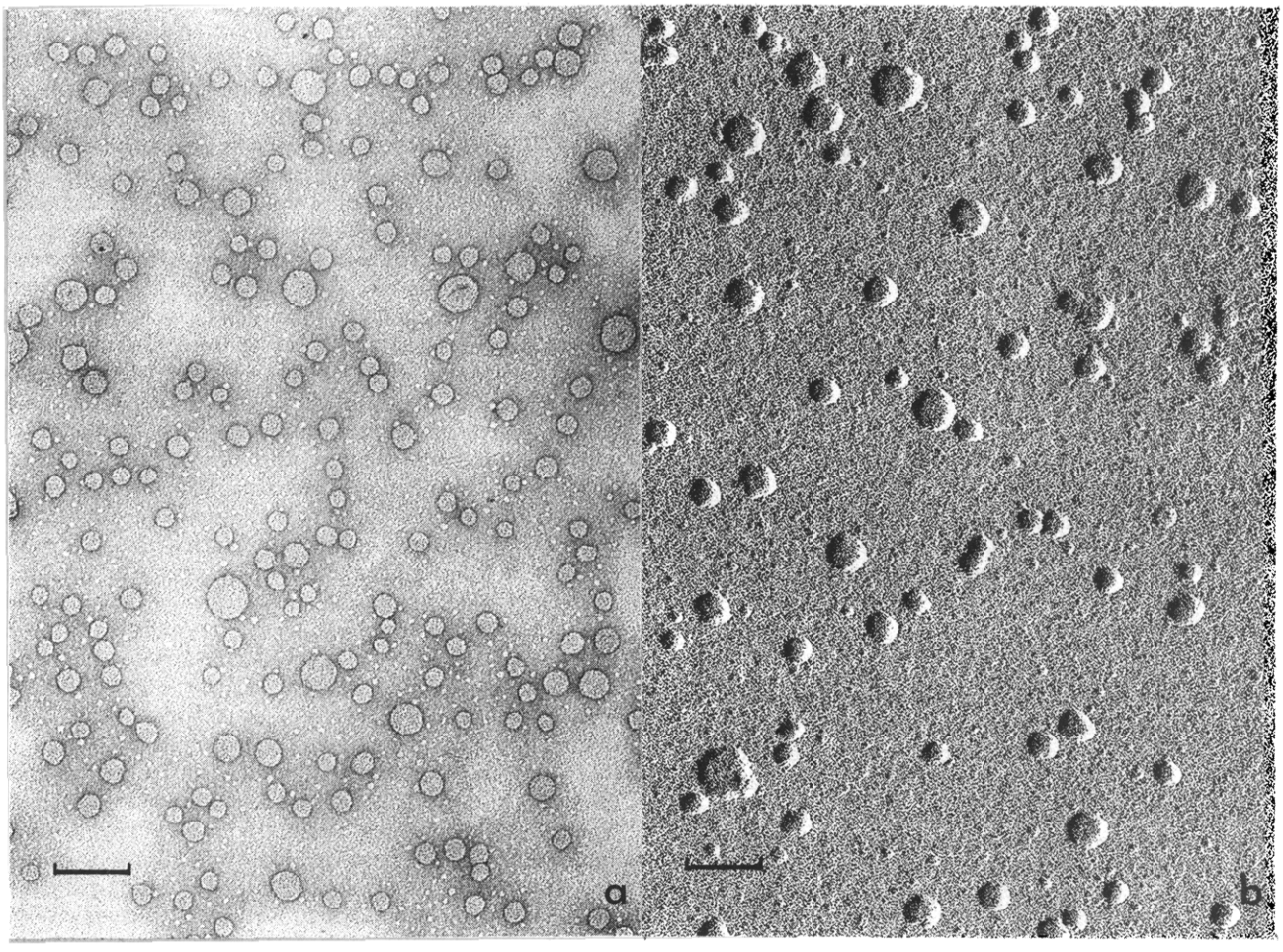

FIGURE 1: (a) Negatively stained preparation of osmium-fixed phospholipid vesicles. The vesicles contain 4 mol % PA and 96 mol % PC. (b) Platinum-shadowed preparation of phospholipid vesicles containing 1 mol % PA and 99 mol % PC affixed to polylysine-coated grids. Magnification of both panels, ×100 000. The reference bar corresponds to 1000 Å.

spin-label in the system, we constructed a sample cell which has two separate fluid compartments side-by-side. The cell consists of two quartz capillary tubes (1.1-mm i.d. and 2.2-mm o.d.) bound together and secured in the cavity such that the side-by-side tubes have the same orientation as the Varian quartz flat cell. The capillaries extend from both sample cell mountings at the top and bottom of the cavity and are attached to syringes to facilitate compartment filling with the cell fixed in the cavity and klystron power maintained at ~10 mW (i.e., fixed cavity tune).

The operational symmetry of the dual sample cell was verified by recording and subsequently superimposing spectra of identical samples (against buffer blanks) in each of the two capillary chambers of the cell.

Measurement of Flipping Rates of Membrane-Associated Spin-Label 1. Determinations of flipping to the inner half of the bilayer were carried out by an approach similar to that taken by Kornberg and McConnell (1971). Sonicated phospholipid vesicles and stock spin-label 1 were mixed at room temperature to give final concentration of 1.9% (w/v) lipid and 2×10^{-5} M spin-label 1. At specified time points after mixing, 300-μl aliquots were removed and cooled to 0 °C in an ice–water bath and 15 μl of 55 mM ascorbate (pH 7.0) was added (final concentration 2.5 mM) to reduce spin-label in the bulk solution and external bilayer surface. In preliminary experiments, this level of ascorbate was verified to completely reduce all available nitroxide in less than 3 min at 0 °C. Reduced samples were rapidly transferred to the Varian flat cell, placed in the EPR cavity, and maintained at 0 ± 0.1 °C with a stream of temperature-regulated nitrogen gas entering through the cavity irradiation window. At no time did the sample, cooled before placement in the spectrometer, reach a temperature above 12 °C, and cooling to 0 °C was achieved in 3–4 min after introducing the sample into the cell and the EPR cavity. The spectra of samples were recorded 10 min after mixing with ascorbate, and the amplitude of the remaining EPR signal was used to determine the amount of spin internalized as a result of flipping.

Results

Vesicle Size and Surface Charge. Typical dispersions of phospholipid vesicles, prepared by sonication, are depicted in Figure 1. The left panel shows vesicles fixed with OsO_4 and negatively stained with uranyl acetate, while the right panel shows fixed vesicles adsorbed to a polylysine surface and shadowed with a thin layer of platinum. Measurements of vesicle size distributions were made on micrographs of magnification 112 000 and the frequencies were recorded for 18 Å increments in diameter. The results are reported in Table II. With regard to the actual vesicle diameters in aqueous suspension, we remain uncertain as to the extent of vesicle flattening incurred in preparing samples for microscopy. In all cases, the weighted-average diameter is larger than the most frequently observed diameter, indicating that the distribution

TABLE II

Vesicle Type Mol % PA	Morphologic Preparation	Most Frequent[a] Vesicle Diameter	Weighted Average[b] Vesicle Diameter	
1 mol %	Platinum shadowing	355	400	(s = 110)
	Negative staining	345	375	(s = 95)
2 mol %	Platinum shadowing	290	325	(s = 100)
	Negative staining	270	315	(s = 65)
4 mol %	Platinum shadowing	285	330	(s = 95)
	Negative staining	270	305	(s = 85)

[a] The most frequent diameter represents the center value of the appropriate 18-Å increment of measured diameter rounded off to the nearest 5 Å. [b] The weighted average vesicle diameter values have also been rounded off to the nearest 5 Å. The standard deviation is given as an s-value in parentheses.

is asymmetric, being skewed toward larger diameters. Also, vesicles of lower magnitude surface potential tend to be larger than those of higher magnitude (compare the weighted-average diameter of 1 mol % PA-containing vesicles to 2 and 4 mol % PA-containing vesicles). A small, but significant, fraction of the vesicles have diameters greater than 480 Å, this fraction being most prevalent for vesicles containing 1 mol % PA.

If 280 Å is taken as a representative, actual vesicle outer diameter, with a bilayer thickness of 50 Å, calculations presented under Appendix, part A show that there are approximately 5000 phospholipid molecules/vesicle. From the ratio, outer surface area:inner surface area of the vesicle, ~70% of the phospholipid molecules are present in the outer leaflet of the bilayer. Thus, approximately 3500 phospholipid molecules constitute the external surface of a 280-Å diameter vesicle. For vesicles containing 1, 2, 4, and 8 mol % PA used for surface potential measurements, 35, 70, 140, and 280 molecules, respectively, of PA would be expected to be present in this surface, assuming that PA distribution parallels general phospholipid distribution.[3] For future reference, at 2×10^{-5} M spin-labeled amphiphile and 1.9% (w/v) phospholipid routinely used for surface potential measurements, further calculation (see Appendix, part A) indicates that there are a maximum of 4 cationic, spin-labeled amphiphiles per phospholipid vesicle. For 1 mol % PA-containing vesicles in the absence of NaCl, 90% of the amphiphile is membrane associated or ~3.6 molecules/vesicle. Thus, the presence of the probe contributes to a maximum decrease of 10% in the inherent surface charge of the vesicles. At higher PA concentrations, the decrease becomes progressively smaller.

Analysis of Spectra. EPR spectra of spin-label 1 in aqueous solution and in membrane-containing samples with different aqueous salt concentrations are depicted in Figure 2. The spectra in Figure 2b (especially the I = −1 resonance lines) clearly indicate the presence of two spin populations, one vesicle bound (broadened signal) and the other free (sharp signal), the relative proportions being a function of the salt concentration and, thus, suggesting an electrolyte-dependent equilibrium. The latter spectra are considered to be composites representing the simple superposition of spectra of free and bound spin-label 1. The basis for this interpretation is presented in Figure 3. Using the dual sample cell described under Methods, spectra of aqueous spin-label 1 and predominantly membrane-associated spin-label 1 were recorded individually, the superposition of which is shown in Figure 3a. Simultaneous recording of these two samples (Figure 3b) demonstrates the exact summation of the separate components. Comparison of Figure 3b to the spectrum of nearly the same proportions of bulk aqueous and vesicle-associated spin-label 1 *in equilibrium* (Figure 3c) indicates the close similarity in line shape. Thus, we take the spectra (henceforth referred to as composite spectra) to indicate an equilibrium between free and bound spin populations, the exchange frequency of the amphiphile being slow relative to the frequency corresponding to the difference in line widths of the membrane-associated and bulk aqueous peaks of the I = −1 resonance. The well-resolved high-field resonance is, therefore, an indicator of spin-labeled amphiphile residing in the bulk aqueous phase.

The relative proportions of bound and free paramagnetic amphiphile in equilibrium change as a function of aqueous salt concentration reflecting changes in surface potential. The fundamental information required from each spectrum is a measure proportional to the ratio of the number of spin-labeled molecules in each environment. We have extracted these data from composite spectra according to two general methods.

Method 1. Based on the fact that the amplitudes of resonance lines are proportional to the size of the particular spin population, the following procedure is used to derive an amplitude (and, hence, spin population) ratio from composite spectra. (1) The amplitude, peak-to-trough, of the well-resolved, high-field resonance line for aqueous spin is measured (corrected for underlying bound signal based on the known line shape (refer to Figure 2b)). The amplitude will be referred to as $A_{f(-1)}$. (2) An amplitude proportional to the total spin present in the system is determined. Reference to Figure 3 (panels a and b) indicates that the best choice is the trough amplitude of the I = 0 resonance line, where the troughs for membrane-associated and aqueous spin-labeled molecules are nearly coincident (displacement ≤0.4 G). Thus, $A^-_{total(0)} = A^-_{f(0)} + A^-_{b(0)} = k_f n_f + k_b n_b$, where A^- is the amplitude of the trough,[4] n_f and n_b are, respectively, the number of spin molecules free in aqueous solution and bound to the membrane, and k_f and k_b are proportionality constants. (3) To obtain $A^-_{f(0)}$, the measured amplitude of the high field resonance line ($A_{f(-1)}$) must be scaled by a factor which takes account of the inherent amplitude difference of the I = 0 and I = −1 resonance lines. For spin-label 1 in aqueous solution, $A_{f(0)} = 1.12\ A_{f(-1)}$ (refer to Figure 2a). Since the trough represents half the total amplitude of the symmetrical derivative signal, $A^-_{f(0)} = 0.56\ A_{f(-1)}$. (4) The fraction of total amplitude that is con-

[3] Although Michaelson et al. (1973) have demonstrated an enrichment of phosphatidylglycerol and, thus, a higher surface-charge density on the outer surface relative to the inner surface of sonicated vesicles containing 50 mol % phosphatidylglycerol and 50 mol % phosphatidylcholine, theoretical calculations of Israelachvili (1973) indicate that the ratio of the *number* of charges on the outer–inner surface (equal to 2.3 for a vesicle of outer radius 150 Å) is insignificantly different from the ratio of outer–inner surface areas (70/30 = 2.3 for vesicles of the same diameter). Therefore, at low concentrations of charged phospholipid (<10 mol % PA), we assume that PA distribution parallels the ratio of surface areas.

[4] For the amplitude, denoted A, the superscript "−" indicates that the amplitude is measured for the trough only of the resonance line. The subscripts in the notation refer to free, f; bound, b; and total spins. The parenthetically enclosed number, (0) or (−1) identifies the resonance line determined by the nitrogen nuclear-spin quantum numbers, I = 0 and I = −1.

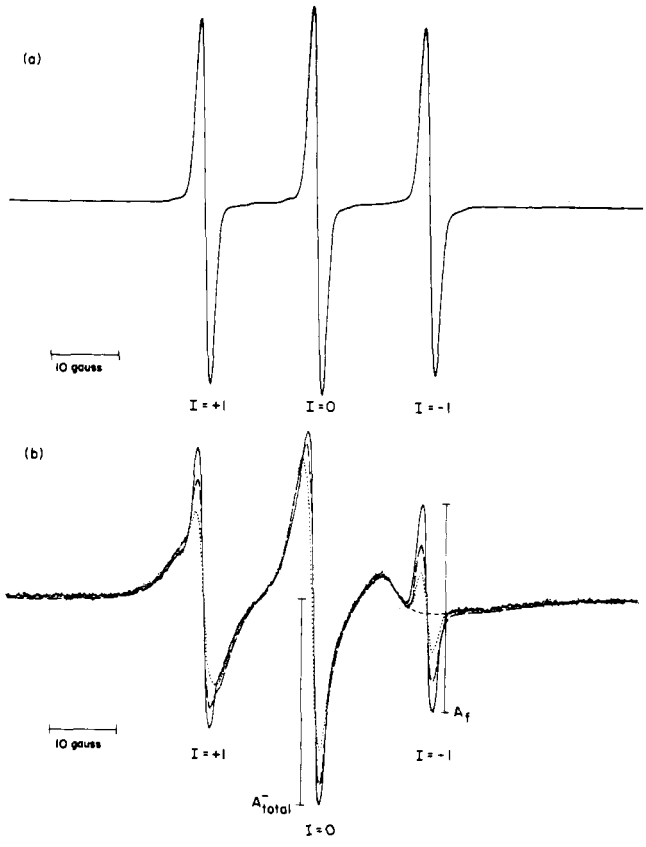

FIGURE 2: (a) EPR spectrum of 2×10^{-5} M spin-label 1 in aqueous solution. Note that the amplitudes are different for each of the three resonance lines, I = +1, I = 0, I = −1. (b) Spectra of 2×10^{-5} M spin-label 1 in the presence of phospholipid vesicles containing 8 mol % PA and suspended in 400 mM (—), 50 mM (- -), or in the absence (• • •) of NaCl. The NaCl concentrations span the range used for surface potential measurements. The I = −1 resonance line shows a well-resolved sharp (aqueous) signal, the amplitude of which, designated A_f, varies with salt concentration. Based on the known line shape for the broadened signal a baseline (- - -) has been provided for the sharp signal. The trough of the I = 0 resonance line has been designated A^-_{total}, since it is used as a measure of total spin-label 1 for the calculation of distribution coefficients.

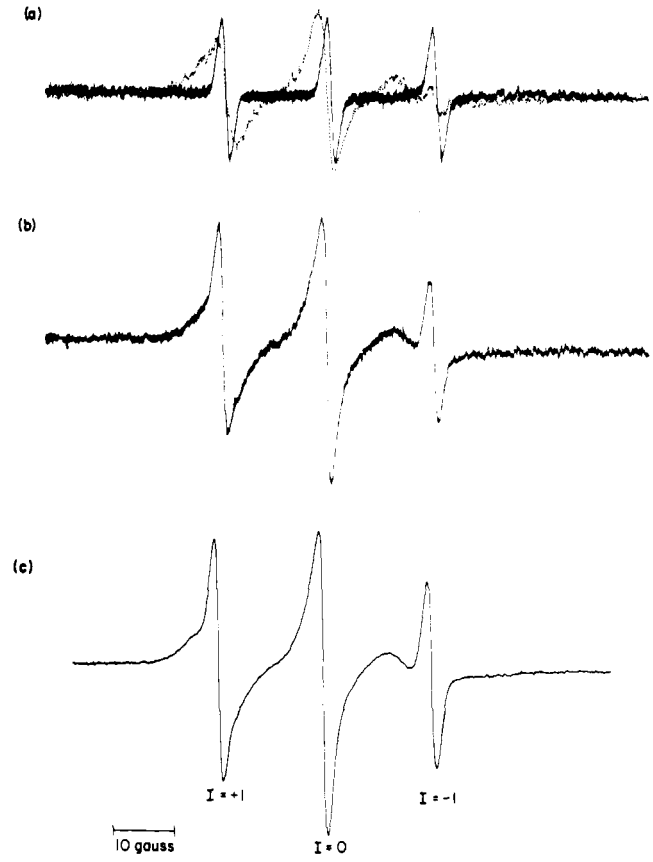

FIGURE 3: EPR spectra obtained using the dual sample cell comprising two quartz capillary tubes mounted side-by-side. (a) The superposition of spectra recorded individually for 4×10^{-6} M aqueous spin-label 1 (—) and 2×10^{-5} M spin-label 1 in the presence of 4 mol % PA-containing vesicles (• • •), where the bulk of the spin-label is membrane associated. (b) The spectrum recorded with both of the above samples present in the cavity simultaneously. Manual summation of the individual spectra in 3a gives this same spectrum. (c) EPR spectrum for a sample representing the equilibrium between nearly the same proportions of aqueous and bound spin-label 1 recorded in the single compartment Varian flat cell. The close similarity in line shape between 3b and 3c provides the basis for treating composite spectra as the superposition of spectra for two spin populations—free and bound.

tributed by aqueous spin-label is calculated as $A^-_{f(0)}/A^-_{total(0)}$, and the fractional amplitude of membrane-associated spin-label $A^-_{b(0)}/A^-_{total(0)} = 1 - (A^-_{f(0)}/A^-_{total(0)})$. The ratio of the latter to the former of these fractional amplitudes yields $A^-_{b(0)}/A^-_{f(0)}$ which, from above, is equal to $k_b n_b/k_f n_f = \beta(n_b/n_f)$. Thus, the ratio of the number of nitroxide-labeled amphiphile molecules in each environment is reflected in an amplitude ratio for bound:free spin.

This method of data reduction is based on the assumption that spectral changes result only from population changes and not from line shape changes. For the signal arising from membrane-associated nitroxide, we have verified that line shape is independent of the concentration of spin-label 1. At concentrations of 1×10^{-4} M or less, the measured amplitude ratio $A^-_{b(0)}/A^-_{total(0)}$ from composite spectra is independent of spin concentration for 4 mol % PA-containing vesicles suspended in 1 mM phosphate buffer. Furthermore, under conditions where nearly all of the amphiphile is membrane associated (at 4 and 8 mol % PA), the identity of spectra taken of vesicles of distinct inherent surface charge (PA concentration), but prepared at the same surface potential by adjusting the bulk NaCl concentration, indicates that intrinsic line shapes are not a function of PA content or NaCl concentration.

For the signal arising from aqueous spin-label 1, line shape is independent of salt concentration over the range routinely used in surface potential titrations (0–400 mM). The hyperfine coupling constant in all cases is 16.76 ± 0.06 G. Fluctuations in this parameter are produced only at exceedingly high salt concentrations (Hamilton and McConnell, 1968). Finally, exchange broadening of the signal was not detectable at an aqueous concentration of spin-label 1 of 2.5 mM, which exceeds the maximum concentration expected at the vesicle surface.[5]

Method 2. The second general approach to determining the equilibrium distribution of spin-label from the composite spectra (Figure 2b,c) is based on the direct determination of the number of molecules of spin-label 1 present in each phase. We have carried out this measurement in two ways.

Using aqueous solutions of 2×10^{-5} M spin-label 1, we have calibrated the amplitude of the high-field resonance line in units of nanomoles of spin-label. For vesicle-containing samples with the same total amount of spin, the amount of aqueous spin

[5] The upper limit of surface potentials investigated here is ~100 mV. At 2×10^{-5} M spin-label I, the maximum surface concentration is estimated as $c_{max} = (2 \times 10^{-5})e^{-\psi ZF/RT} \simeq 1$ mM.

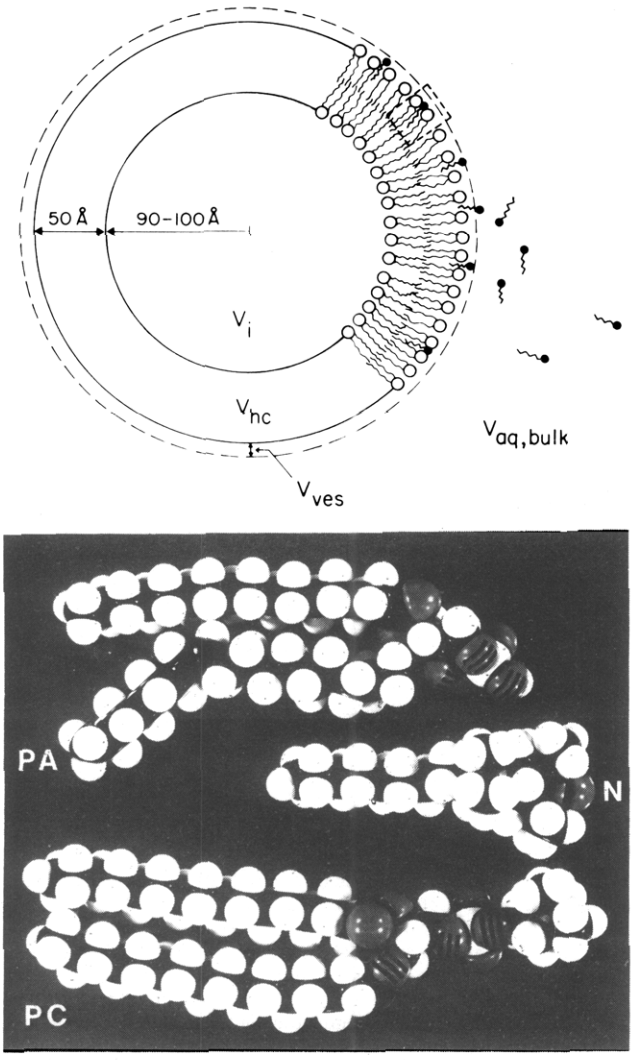

FIGURE 4: Schematic drawing and space-filling models indicating the equilibrium and likely mode of association of spin-label I with the membrane. In the drawing, the aqueous interior volume of the vesicle has been labeled V_i; the volume of the hydrocarbon phase of the membrane, V_{hc}; the volume of the aqueous surface phase occupied by the nitroxide of membrane-associated spin label I, V_{ves}; and the volume of bulk aqueous solution, $V_{aq,bulk}$. The amphiphile is designated by a small filled circle with a short-pleated tail. Spin-label residing within V_{ves} gives rise to a partially immobilized signal. The alkyl chain of the probe penetrates into the nonpolar interior of the membrane to the level of the 5th or 6th carbon of the phospholipid fatty acid chains, as indicated by the space-filling models. Penetration of the quaternary ammonium group of spin-label I below the level of the lipid–glycerol backbone is unlikely (Parsegian, 1969) and indicates the inner boundary of the vesicle phase. The quaternary ammonium is thus placed at the level of the phospholipid phosphate, while the nitroxide extends to the level of the PC choline head groups. When the quaternary ammonium group is located external to the choline nitrogens, motion is expected to be too rapid to generate partially immobilized spectra. This view is supported by the relatively sharp EPR spectrum obtained at room temperature for bilayers containing PC spin-labeled on the choline nitrogen. Thus, the region of the choline nitrogens is taken as an outer limit to the vesicle phase. V_{ves} is, thus, the volume of this thin shell ~10 Å thick surrounding each vesicle and corrected for the excluded volume of the phospholipid headgroups.

is measured directly in nanomoles as the amplitude of the I = −1 aqueous signal in the composite spectrum. Since the prepared sample contains a known total amount of spin-label I, the quantity of membrane-associated label is obtained by difference. Thus, the phase population ratio n_b/n_f is expressed directly. Since this method is based on absolute magnitudes of peak heights and not ratios of the peak heights, the measurements are anticipated to be sensitive to the reproducibility of tuning of the EPR spectrometer, the linearity of the instrument's signal amplifier, and the reproducibility in preparing samples.

Another drawback in determining population ratios from measurements of absolute peak amplitudes (rather than peak ratios) is that the total spin concentration must be insured to remain constant. Nitroxide probes often undergo substantial reduction in the presence of biologic membranes (Kury and McConnell, 1975; Kornberg et al., 1972). However, with freshly prepared vesicles containing PC and PA, we observe a near constancy in total spin-label concentration for a period of at least 6 h after preparation of the vesicles. Thus, this method provides a convenient test of the more generally applicable peak ratios method of calculating population ratios.

The number of moles of spin-label I present in each phase was also determined from values of aqueous and total spin intensity obtained from twice-integrated EPR spectra. Composite spectra for each surface charge and salt concentration were recorded on magnetic tape and integrated by standard computer techniques. The resulting absorption spectra (scaled and plotted) were integrated a second time by planimetry to obtain areas proportional to total- and free-spin populations, the latter taken as three times the area of the absorption peak due to the high field resonance of the free spin. By analogy to part 4 of Method 1, the area fraction of free spin was used to calculate the ratio of bound to free spin, n_b/n_f. As will be subsequently shown, the primary intent of determining n_b/n_f by integration is to corroborate the measurements obtained directly from the first derivative spectra, the latter method being preferred because of its simplicity.

Thermodynamic Analysis of the Equilibrium. The distribution of spin between the external vesicle surface and the bulk solution is treated as a simple phase equilibrium. The membrane surface phase is considered to have a well-defined volume per gram of lipid, $\bar{V}_{ves}$. Operationally, this volume is unambiguously defined as that volume per gram of lipid occupied by spin-labels giving rise to a bound (partially immobilized) signal. Furthermore, $\bar{V}_{ves}$ is taken to be a constant independent of surface charge density and ionic strength. For any vesicle preparation, the total volume of the vesicle phase is $V_{ves} = m_l\bar{V}_{ves}$, where m_l is the mass of lipid. The volume of the bulk aqueous phase available to the spin-label, V_{aq}, is defined as $V_{aq} = m_{aq}\bar{V}_{aq}$, where m_{aq} is the mass of solvent external to the vesicle surface phase and $\bar{V}_{aq}$ is the partial specific volume of the solvent. The definitions assume that the spin-label does not sample the internal vesicle membrane surface or aqueous space. The experimental basis for this assumption will be discussed below.

Although not required for a formal analysis, a physically realistic interpretation of V_{ves} and V_{aq} is shown in Figure 4 for a single vesicle.

The electrochemical potentials of the spin-label in the vesicle (membrane) and bulk aqueous phases are defined as,

$$\tilde{\mu}_{ves} = \mu^\circ_{ves} + RT \ln(X_{ves}\gamma_{ves}) + ZF\psi_{ves}$$

$$\tilde{\mu}_{aq} = \mu^\circ_{aq} + RT \ln (X_{aq}\gamma_{aq})$$

where μ°_{ves}, μ°_{aq} are the chemical potentials in the corresponding Henry's law standard states for each phase in the absence of external electric fields and electrolytes; γ_{ves}, γ_{aq} are the single ion activity coefficients in the two phases; X_{ves}, X_{aq} are the mole fractions of the spin-label in the two phases defined such that in each phase, X (label) + X (H_2O) = 1; ψ_{ves}

is the average electric potential within V_{ves} referenced to $\psi = 0$ in the bulk aqueous phase (see below); Z,F,R,T are, respectively, the charge on the spin-label, the Faraday constant, the universal gas constant, and the absolute temperature.

At equilibrium, $\tilde{\mu}_{ves} = \tilde{\mu}_{aq}$ and

$$-\left(\frac{ZF\psi_s}{RT}\right) = \ln\left(\frac{X_{ves}\gamma_{ves}}{X_{aq}\gamma_{aq}}\right) + \left(\frac{\mu^\circ_{ves} - \mu^\circ_{aq}}{RT}\right) \quad (1)$$

The quantity $\mu^\circ_{ves} - \mu^\circ_{aq}$ is the unitary free energy of transfer of a spin-label from the aqueous phase to the vesicle phase, and $-(\mu^\circ_{ves} - \mu^\circ_{aq})/RT = \ln K_0$, where K_0 is the phase partition coefficient (equilibrium constant) for the spin in the absence of a surface potential. The quantity $(X_{ves}\gamma_{ves}/X_{aq}\gamma_{aq}) \equiv K$ is just the equilibrium constant in the presence of a surface potential. Thus, eq 1 may be expressed as:

$$K = K_0 e^{-ZF\psi_s/RT} \text{ or } \psi_s = -\left(\frac{RT}{ZF}\right)\ln\left(\frac{K}{K_0}\right) \quad (2)$$

Equation 2 shows that the surface potential ψ_s of any vesicle may be determined directly by measurement of the spin-label partition coefficient (K) if the value in the absence of surface charge, K_0, is known. In order to obtain values of K and K_0 from spectral data, we assume that deviations of activity coefficients from unity are similar in both phases (i.e., $\gamma_{ves}/\gamma_{aq} \approx 1$) and thus reduce each equilibrium constant to a mole fraction ratio. With this approximation and in dilute solution of spin-label 1,

$$K = \frac{X_{ves}\gamma_{ves}}{X_{aq}\gamma_{aq}} \simeq \frac{X_{ves}}{X_{aq}} \simeq \left(\frac{n_{ves}}{V_{ves}}\right)\Big/\left(\frac{n_{aq}}{V_{aq}}\right) \quad (3)$$

where n_{ves} is the number of spins in the defined vesicle phase of volume V_{ves}, and n_{aq}/V_{aq} is the number of "free" spins per aqueous volume *external* to the ionic double layer.[6] Recalling that $A^-_{b(0)}/A^-_{f(0)} = \beta(n_b/n_f)$ (method 1 of spectral analysis), eq 3 can be written (taking $n_b/n_f = n_{ves}/n_{aq}$ as discussed in footnote 6).

$$\frac{A^-_{f(0)}}{A^-_{b(0)}} = \left(\frac{1}{K\beta}\right)\left(\frac{V_{aq}}{V_{ves}}\right) \quad (4)$$

and plots of $A^-_{f(0)}/A^-_{b(0)}$ vs. V_{aq}/V_{ves} at a constant ψ_s are expected to be linear. The slopes of such plots at different values of ψ_s then yield relative values of K. The variable V_{aq}/V_{ves} is easily manipulated by changes in vesicle concentration, and is expressed in terms of experimentally accessible quantities according to the following equation, the derivation of which is present under Appendix, part B.

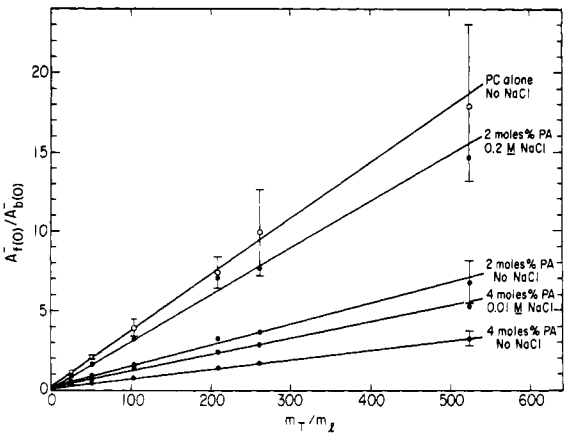

FIGURE 5: The amplitude ratio of free:bound spin-label 1 as a function of the mass ratio m_T/m_{lipid}. Phospholipid vesicles comprising pure PC or the specified PA content at final lipid concentrations of 3.80, 1.90, 0.95, 0.48, 0.38, 0.19% (w/v) were mixed with 2×10^{-5} M spin-label 1 and NaCl at 0, 0.010, or 0.200 M final concentration. The magnitudes of the error bars have been calculated from measured uncertainties of 0.4% in the reproducibility of recording of EPR spectra, 0.5% in the measurement of peak amplitudes, and an estimated maximum error of 10% in sample preparation.

$$\frac{V_{aq}}{V_{ves}} = \left(\frac{\bar{V}_{aq}}{\bar{V}_{ves}}\right)\left[\left(\frac{m_T}{m_l}\right) - Q\right] \quad (5)$$

where: m_T/m_l is the ratio of the total solvent mass to the total mass of lipid in a sample; $\bar{V}_{aq}$ and $\bar{V}_{ves}$ are as defined previously; Q is a constant (defined under Appendix). Equation 4 may then be written as:

$$\frac{A^-_{f(0)}}{A^-_{b(0)}} = \left(\frac{1}{K\beta}\right)\left(\frac{\bar{V}_{aq}}{\bar{V}_{ves}}\right)\left[\left(\frac{m_T}{m_l}\right) - Q\right] \quad (6)$$

Plots of $A^-_{f(0)}/A^-_{b(0)}$ vs. m_T/m_l for vesicles containing different amounts of PA and suspended in different NaCl concentrations are shown in Figure 5. The plots are linear and, according to eq 6, are expected to have slopes and intercepts of $(\bar{V}_{aq}/\bar{V}_{ves})(1/K\beta)$ and $(-Q/K\beta)(\bar{V}_{aq}/\bar{V}_{ves})$, respectively. Also included are data for vesicles containing PC alone, the zero surface potential reference. Error bars representing a combined uncertainty in sample preparation, reproducibility in recording EPR spectra, and measurement of peak amplitudes are included to indicate the variation in the data and are found to be largest at the very low lipid concentrations. Therefore, we routinely carried out surface potential measurements on samples containing 1.9% (w/v) lipid where uncertainties in the intensity ratios are small.

The experiment for vesicles containing PC only was carried out three times, and treatment of the data by the method of linear least-squares indicated an ordinate intercept of 0.0029. The linear equation predicts that the intercept should be negative, since each of the quantities $\bar{V}_{ves}$, $\bar{V}_{aq}$, Q, β, and K is positive. The magnitude of the intercept, however, must be less than 0.03,[7] and we hesitate to interpret such a small discrepancy, although we consistently observed that best linear plots for the data gave positive intercepts which tended toward higher values as the surface potential was increased. Either there is some small systematic error in the manner in which distribution ratios are deduced from the spectra, or an effect such as a small but finite level of flipping of spin-label 1 to the

[6] Rigorously, the volume V_{aq} in eq 3 is not the same as that defined in Figure 4, and should be taken as the volume of bulk solution excluding the principal volume of the double layer. However, in all but the most extreme dilutions of NaCl, the Debye lengths are sufficiently short to allow V_{aq} of eq 3 to be closely approximated by the total aqueous volume.

The sharp EPR resonance due to free spin contains contributions from *all* free spin, including those within the double layer. Since the volume of the double layer is usually a small fraction of the total solution volume, and because of the large excess of sodium ions relative to the spin-label cation, the free spin in the double layer is a negligible contribution to the total free spin for the surface charge densities and ionic strengths considered here. As an excellent approximation, the number of free spins determined from the EPR spectra (n_f) will be identified with n_{aq} in eq 3, and $n_b/n_f \simeq n_{ves}/n_{aq}$. Inaccuracies incurred by this approximation become significant only for the higher surface-charge densities (4 and 8 mol % PA) at extreme dilution of NaCl, where the fraction of excess charge in the double layer due to the spin-label becomes significant. In these limiting cases, the maximum error contributed by this source to the derived surface potential amounts to ca. 10–15%. It should be pointed out that this error in very dilute salt solutions is, to a large extent, canceled by the approximation error in V_{aq} under these same conditions.

[7] $\bar{m}_l$, $\bar{m}_{ves}$, $\bar{V}_{ves}$ (see Appendix, part B) are all of the order of unity; experimentally, $\beta \simeq 0.15$, while K varies with surface potential but is ≥ 500. Thus, $-0.03 \leq$ intercept ≤ 0.

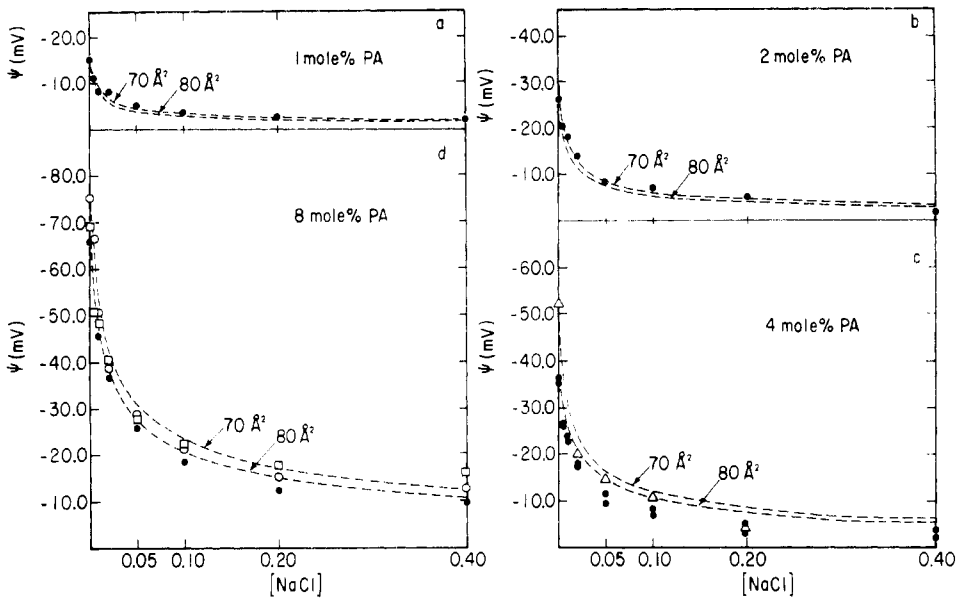

FIGURE 6: The surface potential of phospholipid vesicles as a function of salt concentration. Surface potentials were calculated for each of the four types of vesicle preparations (1, 2, 4, and 8 mol % PA) from measured amplitude ratios using eq 7 and are indicated by filled circles (●). For vesicles containing 4 mol % PA, data (△) are included for potentials calculated according to eq 9 using values of slopes of the type presented in Figure 5. For 8 mol % PA-containing vesicles, surface potentials calculated from ratios n_b/n_f, determined both by calibration of the amplitude of the $I = -1$ resonance line (□) and by double integration of derivative spectra (○), are presented. The two broken lines in each panel indicate potentials calculated according to the Gouy equation assuming an average area/phospholipid of 70 or 80 Å^2.

inner half of the vesicle bilayer may explain this observation.

The Calculation of Surface Potentials. Most experimental determinations of surface potential were carried out by taking spectra of a series of vesicle samples at a fixed total lipid concentration 1.9% (w/v) in which the PA concentration (and thus the surface charge) was fixed while the NaCl concentration was varied from 0–0.400 M. The resulting phase distribution measurements, derived from the spectra in three independent manners (described under analysis of spectra and enumerated below), were used individually to calculate surface potentials using the appropriate form of eq 2.

Details of the following equations for surface potential calculation from individual phase distribution measurements are presented under Appendix, part C. (1) Where amplitude ratios, $A^-_{b(0)}/A^-_{f(0)}$, are derived from the magnitude of the aqueous and total signals of the I = 0 resonance trough:

$$\psi_s = -\left(\frac{RT}{ZF}\right)\left\{\ln\left(\frac{A^-_{b(0)}}{A^-_{f(0)}}\right) + \ln\left(\left(\frac{m_{aq}}{m_l}\right)\left(\frac{1}{\alpha_0}\right)\right)\right\} \quad (7)$$

where m_{aq} is the mass of bulk solvent, external to the vesicle, m_l is the mass of lipid, and α_0 is the inverse slope of the plot of $A^-_{f(0)}/A^-_{b(0)}$ vs. m_T/m_l for the PC reference. In practice, $m_{aq} \simeq m_T$ and this approximation may be used in eq 7 and 8 below with little error. (2) Where spin-label distribution ratios, n_b/n_f, are derived from nanomole calibration of the magnitude of the aqueous high field ($I = -1$) resonance line (Method 2 under analysis of spectra):

$$\psi_s = -\left(\frac{RT}{ZF}\right)\left\{\ln\left(\frac{n_b}{n_f}\right) + \ln\left(\frac{m_{aq}\beta}{m_l\,\alpha_0}\right)\right\} \quad (8)$$

with m_{aq}/m_l and α_0 as above, and $\beta = k_b/k_f$. The constants k_f and k_b are determined on the day of the experiment from a total aqueous amphiphile standard and a high surface potential vesicle sample (where the amphiphile is maximally membrane associated). (3) Where distribution ratios are determined from doubly integrated spectra, the equation relating ψ_s to the measured n_b/n_f, as discussed under Appendix, part B, is identical to eq 8.

A fourth calculation of ψ_s, also based on eq 2, is afforded by experiments comprising the phase distribution measurements as a function of systematic variation of the total weight concentration of lipid (eq 6). For this latter calculation,

$$\psi_s = -\left(\frac{RT}{ZF}\right)\ln\left(\frac{\alpha}{\alpha_0}\right) = -\left(\frac{RT}{ZF}\right)\ln\left(\frac{K}{K_0}\right) \quad (9)$$

where $\alpha \equiv K\beta(\bar{V}_{ves}/\bar{V}_{aq})$ and $\alpha_0 \equiv K_0\beta\,(\bar{V}_{ves}/\bar{V}_{aq})$ are just the inverse slopes of $A^-_{f(0)}/A^-_{b(0)}$ vs. m_T/m_l plots (Figure 5) for the chosen experimental sample (fixed surface charge plus fixed salt concentration) and the zero surface charge (PC in buffer) reference, respectively.

Figure 6 presents the results of determinations of ψ_s as a function of NaCl concentration from amphiphile distribution data obtained for four types of phospholipid vesicles containing 1, 2, 4, and 8 mol % PA. The data in each panel are supplemented by curves which indicate the potentials predicted by the Gouy equation $\psi_G = (2kT/e)\,\sinh^{-1}\,(\sigma/c^{1/2})(500\pi/DRT)^{1/2}$ at two different assumed surface charge densities, σ, calculated using molecular areas of 70 Å^2 and 80 Å^2 per phospholipid. In this expression, k, R, and D are the Boltzmann, universal gas, and aqueous dielectric constants respectively; T, the absolute temperature; e, the unit electronic charge; and c, the molar ionic concentration (Verwey and Overbeek, 1948; Davies and Rideal, 1963).

In determining the ionic concentration, we have taken into account the concentration of counterions of PA, the amount of NaOH used to neutralize the vesicle preparations before use, the 1 mM phosphate buffer at pH 7, and the NaCl concentration.

From Figure 6 it is obvious that the dependence of surface potential on NaCl concentration is, to a close approximation, the same as that predicted by the Gouy equation, and the absolute magnitudes of the surface potentials are nearly coincident with ψ_G (70 Å^2/molecule) for vesicles containing 1 and

2 mol % PA. There is also striking agreement of the surface potential profiles measured experimentally for vesicles containing 8 mol % PA and calculated according to the Gouy equation (80 Å^2/molecule). Although predicted and measured surface potential profiles for 4 mol % PA-containing vesicles exhibit the same shape, there is a small but significant (~4 mV) systematic difference between the calculated (80 Å^2/molecule) and experimental values of the surface potential.

All independent methods for determining ψ_s as a function of NaCl concentration are in reasonable agreement. Thus, the simple use of amplitude ratios for bound:free spin-label 1 for estimating surface potentials is entirely acceptable and, in fact, proves to be the method of choice, since it automatically normalizes for variations in total spin concentration and other fluctuations, and shows the least scatter from a smooth curve of best fit. As shown by the two distinct experiments presented for 4 mol % PA-containing vesicles (Figure 6c), the values of surface potential are reproducible to within 10% at potentials more negative than −10 mV. The reproducibility for vesicles having surface potentials of magnitude lower than 10 mV should improve if precautions are taken to maintain a reproducible temperature while taking spectra and, as the subsequent discussion of amphiphile flipping rate indicates, to measure phase distributions of vesicle preparations at a standardized time after introduction of the label.

The fact that the absolute magnitudes of ψ_s obtained by the method of choice (eq 7) are consistently slightly lower than obtained by the other methods described may reflect the very slight (0.4 G) discoincidence in the troughs of the I = 0 resonance lines for membrane-associated and free paramagnetic amphiphile.

The relationship between ψ_s and ψ_G is presented in a different manner in Figure 7. The solid line in each panel is drawn with a slope of unity, and it is clear from the figure that $\psi_s = \psi_G \pm \Delta\psi$, where $\Delta\psi$ is a small constant, and is a measure of any systematic difference between the theoretical and experimental surface potentials. Thus, $(\partial\psi_G/\partial c)_{\sigma,T} = (\partial\psi_s/\partial c)_{\sigma,T}$ for all values of c (the NaCl concentration) and the experimental and theoretical curves of ψ vs. c have the same shape, irrespective of the absolute magnitudes of the potentials.

The practical significance of this result may be seen by equating the expressions for the appropriate concentration derivatives of ψ_G and ψ_s (from eq 7) to give

$$\sigma^2 = (1.28 \times 10^9)\left(\frac{\partial \ln \lambda}{\partial c}\right)_{\sigma,T}^2 \Big/ \left\{\left(\frac{1}{c^3} - \frac{1}{c}\right)\left(\frac{\partial \ln \lambda}{\partial c}\right)_{\sigma,T}^2\right\}$$

where $\lambda = A^-_{b(0)}/A^-_{f(0)}$ and the numerical values of physical constants have been substituted for a temperature of 22 °C (σ in esu/cm^2). Thus, σ may be estimated simply from the dependence of λ on c without any knowledge of the constant terms (β, K_0, m_{aq}/m) involved in eq 7. This result will be useful in biological membrane systems where K_0 is difficult to determine. Furthermore, relatively small errors in the constant terms of eq 7 lead to substantial systematic errors in ψ_s, but such errors do not influence the derived value of σ^2.

Osmotic Effects on Phospholipid Vesicles. Another interesting application of the amphiphile phase distribution is the detection of internal volume changes in vesicles. If the amphiphile is trapped within the vesicle internal space, the resulting equilibrium spin distribution between the internal volume and internal membrane surface will change with changes in the internal volume. In one experiment of this type, vesicles containing interiorized amphiphile were prepared by sonication in its presence followed by ascorbate reduction of the external spin. When these vesicles were subjected to hypertonic sucrose (1 M), a 37% decrease in free spin was observed, indicating a substantial decrease in internal volume.

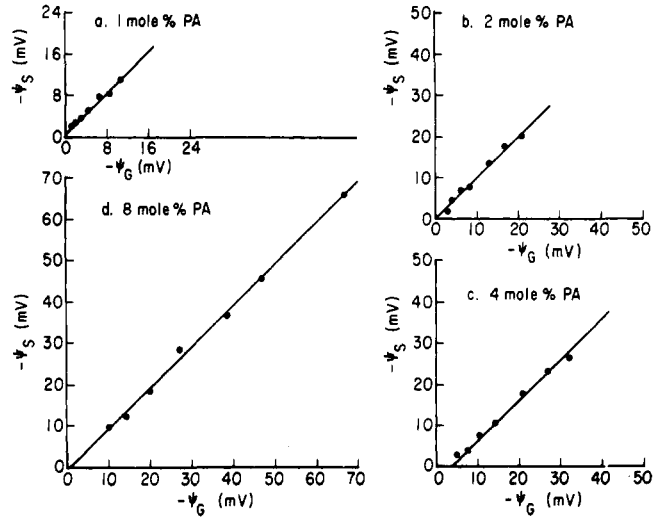

FIGURE 7: Correlation between the theoretical (ψ_G) and experimental (ψ_s) surface potentials. Each panel is a plot of the experimental potential vs. its theoretically predicted value at a fixed surface charge and variable NaCl concentration. The data are replotted from Figure 6. The solid lines are drawn with a slope of unity. For 1 and 2 mol % PA, ψ_G was calculated from σ corresponding to 70 Å^2/phospholipid; for 4 and 8 mol % PA, ψ_G was calculated from σ corresponding to 80 Å^2/phospholipid. The reasons for these choices of area are found under Discussion.

The Kinetics of Transmembrane Migration of Spin-Label 1. The determination of surface potentials by the methods described above implicitly assumes that the bound spin-label 1 resides only on the outer membrane surface. If transmembrane movement of the amphiphile occurred to a significant extent during the experiments, it would effect an overestimate of the equilibrium constant K as defined in eq 3.

Measurements of the spin "flipping" rate (from spectra recorded at 0 °C following the ascorbate reduction) were carried out for several vesicle preparations. In quantitating internalized nitroxide, we assume that the contribution of spin-label 1 present in V_i, the *aqueous* interior of the vesicle (Figure 4) is at all times negligible (the internal volume is very small and the equilibrium constant for association with the inner half of the bilayer is high even at 0 °C). Thus, the total amplitude of the I = 0 resonance line after ascorbate reduction may be used for quantitation and can be related to the amount of internal spin-label by a single constant.

To follow the first-order approach to equilibrium of transmembrane migration of spin-label 1, we used freshly prepared vesicles containing 4 mol % PA suspended in the absence of NaCl. Although, in reality, not quite all of the amphiphile is membrane associated at the onset, we assume complete membrane association (K equal to infinity) with the intent of predicting a minimum half-time of internalization. The rate equations are then similar to those presented by Kornberg and McConnell (1971) for flipping of tempoyl-PC:

$$\ln\left(1 - \frac{n_i}{n_i^{eq}}\right) = \ln\left(1 - \frac{A_i}{A_i^{eq}}\right) = -\left(1 + \frac{S_i}{S_0}\right)kt = -k't \quad (10)$$

n_i, n_i^{eq} indicate, respectively, the number of moles of spin-label 1 present on the inner surface of the vesicle bilayer at time t and at equilibrium (At, $t = 0$, $n_i = 0$). A_i and A_i^{eq} are the corresponding signal amplitudes (experimentally measured); S_i and S_0 are the inner and outer membrane surface areas,

respectively; k is the true first-order rate constant.[8] A plot of experimental data, according to eq 10, is linear over 6 h with a slope, k', equal to 1.2×10^{-3} min^{-1}. This corresponds to a minimal expected half-time of ~580 min for the approach to equilibrium of amphiphile transmembrane migration. k, the true first-order rate constant, is (from k') equal to 0.8×10^{-3} min^{-1}.

To estimate the maximal effect that flipping could have on the magnitude of the surface potential for vesicles containing PA and PC, we use the above kinetic data ($t^{1/2}$ = 580 min) to calculate that a fraction 0.075 of the total spin-label 1 is internalized at t = 4 h (the most frequent duration of phase distribution measurements). The result is a decrease in total spin in equilibrium with the external surface by an amount corresponding to the internalized spin-label 1. Since the external phase equilibrium is always maintained, the ratio n_b/n_f becomes dependent on the amount of internalized spin (n_i) and is given by $n_b/n_f = [n_i + f_m(0)(n_T - n_i)]/[(1 - f_m(0))(n_T - n_i)]$ where $f_m(0)$ is the fraction of total spin (n_T) that is bound at $t = 0$ ($f_m(0) \equiv n_b/n_T$; refer to Table III below). At t = 4 h, we calculate that the increase in n_b/n_f due to flipping results in a maximum overestimate of 6% in the derived surface potential. In each experimental series of surface potential estimates at fixed inherent surface charge, we consistently took spectra of the high magnitude potential samples first. Thus, only the measurements of vesicles having low magnitude surface potential (high NaCl concentration) should be affected to a level approaching 6%.

When eq 10 is reexpressed in exponential form, values of A_i are readily calculated as a function of time after the onset of transmembrane migration. Plots of the *calculated* A_i vs. t are, to a close approximation, linear up to 60 min. Thus, the initial transmembrane migration process can be satisfactorily treated according to zero-order kinetics. For the first 60 min,

$$\frac{dA_i}{dt} \simeq \delta \left(\frac{S_i}{S_0}\right) n_T k f_m(0) = k^\circ \qquad (11)$$

where δ is the constant relating peak amplitude to internal spin-label 1 determined from a spectrum recorded at 0 °C for vesicles containing 4 mol % PA suspended in 1 mM phosphate buffer; S_i, S_0, n_T, and $f_m(0)$ are as previously defined; k is, again, the true first-order rate constant; and k° is the pseudo-zero-order rate constant. Measurements of $\Delta A_i/\Delta t$, then, provide k° which, in turn, may be used to obtain k from the known values of δ, n_T, $f_m(0)$, and (from microscopy) S_i/S_0. The results for vesicle preparations, analyzed in this manner, are presented in Table III. The value of k for 4 mol % PA-containing vesicles in the absence of NaCl (0.8×10^{-3} min^{-1}) is in complete agreement with the value obtained from the rate of approach to equilibrium. Thus, the two kinetic analyses are mutually consistent.

Of further note in Table III, the estimated first-order rate constants are quite similar for the three preparations so analyzed, and the magnitude of k does not correlate with the concentration of PA. Also, the aged preparation of vesicles containing 4 mol % PA in the absence of NaCl translocates spin-label 1 at a rate over five times greater than that found for freshly prepared vesicles. Increase in the rate of tempoyl-PC flip-flop observed with vesicles 2–3 days old (instead of fresh) has been observed by Kornberg and McConnell (1971). For this reason, our surface potential estimates have been made on vesicles which are a maximum of 24 h old and have been sonicated within 3 h of use. Finally, substitution for PA with dicetyl phosphate causes a dramatic increase in the rate of flipping; spin-label 1 is internalized more than ten times faster over the first 60 min after mixing vesicles. In fact, the half-time for approach to equilibrium is 40 min. Thus, for vesicles containing dicetyl phosphate, the inner vesicular surface would contribute substantially to the magnitude of the surface potential where measurements are taken over the course of 4–5 h.

TABLE III: Kinetics of Spin-Label 1 Transmembrane Migration.

Sample	$\frac{\Delta A_i}{\Delta t}$[a]	$f_m(0)$	k (min^{-1})[b]
4 mol % PA vesicles, no NaCl, 3-h old	3.8×10^{-3}	0.945	0.8×10^{-3}
4 mol % PA vesicles, 0.2 M NaCl, 24-h old	0.8×10^{-3}	0.860	0.2×10^{-3}
1 mol % PA vesicles, no NaCl, 40-h old	1.9×10^{-3}	0.888	0.4×10^{-3}
4 mol % PA vesicles, no NaCl, 12-days old	20.0×10^{-3}		
4 mol % dicetyl phosphate vesicles, no NaCl, 40-h old	$>40.0 \times 10^{-3}$		

[a] The ΔA_i values have been taken as the amplitude differences for 5- and 60-min time points. An indication of "greater than" has been placed in front of the value of $\Delta A_i/\Delta t$ for dicetyl phosphate, since a time point of 90 min (past the time satisfactorily described by zero-order kinetics) was used in the absence of data at 60 min. [b] k is calculated using n_T = 12.5 nmol, S_i/S_0 = 0.43, and a value for δ determined at the same instrumental settings used for determination of ΔA_i; in this experiment, δ = 0.9 cm/nmol.

Discussion

We have developed a procedure for estimating the surface potentials of vesicles consisting of single bilayers of binary mixtures of phospholipids—phosphatidylcholine which is zwitterionic and carries no net charge and phosphatidic acid which carries a single net negative charge at neutral pH. By selecting this model system as preparatory to the application to biological membranes, it has been possible to vary not only the surrounding electrolyte concentration but also the surface charge density in a controlled fashion and thereby verify that the nitroxide cationic probe is reporting changes in surface potential through a phase distribution.

The surface potential probe used in these studies has a number of attractive features. (1) Since its ionic nature is instilled by a quaternary ammonium moiety, its charge is constant and independent of pH, a property not shared by lower amines or carboxylic acids. (2) The permeability of phospholipid bilayers to spin-label 1 is negligible for the 4-h duration of experiments; hence, the phase distribution is restricted to the external aqueous medium and the external half of the bilayer. (3) The zero-potential phase distribution (that is, the equilibrium binding constant) of the probe can be controlled by varying the length of the alkyl chain. (4) EPR spectroscopy has a high sensitivity, enabling paramagnetic probes to be applied at exceedingly low concentrations. Although we used 2×10^{-5} M spin-label 1, 4×10^{-6} M should be satisfactory; the latter level corresponds to a maximum of 400 probe molecules/square micron of surface area at infinite surface potential. (5) Although optical techniques have been used to estimate surface potentials of proteins using indicator dyes at

[8] A_i^{eq} is obtained by assuming that (a) line shapes of internal and external membrane-bound spin-label 1 are similar and (b) membrane-associated label is distributed at equilibrium according to surface area, $A_i^{eq} = 0.30(A_0 + A_i)$. But $A_0 + A_i = A_0(0)$, so $A_i^{eq} = 0.30\,A_0(0)$.

similarly low concentrations (7×10^{-5} M by Moller and Kragh-Hansen, 1975), an outstanding advantage to using EPR spectroscopic techniques on membrane-containing samples is the complete freedom from limitations imposed by optical scattering.

The partition of the probe into the membrane phase and the broadened EPR spectrum indicative of restricted tumbling are, in all likelihood, the result of intercalation of the 9-carbon alkyl chain into the hydrophobic region occupied by the esterified fatty acids.

The equilibrium constant, K_0, for binding of spin-label 1 in the absence of surface potential can be estimated from the slope of the plot of $A^{-}_{f(0)}/A^{-}_{b(0)}$ as a function of m_T/m_l for vesicles containing PC alone (Figure 5). The slope, $(1/K_0\beta)(\bar{V}_{aq}/\bar{V}_{ves})$, is equal to 0.037. Experimental values obtained for β (equal to k_b/k_f) are in the range 0.13–0.18, and $\bar{V}_{ves}$ (for the external surface only) is calculated to be ~0.3 ml of H_2O/g of lipid, based on the volume calculated for a 10 Å shell surrounding each phospholipid vesicle (assumed vesicle radius = 140 Å) and a lipid mass per vesicle of 6.4×10^{-18} g (5000 phospholipid molecules, as under Appendix, part A). K_0 then falls in the range 500–700. Since K is always greater than K_0, the justification for considering K to be large enough to be approximated as being infinite in the analysis of flipping rate is evident.

The value of K_0 is further useful for estimating the molar free energy of transfer of the alkyl chain of the amphiphile between the bulk aqueous and vesicle phases. From eq 1 ($\psi_s = 0$), the free energy of transfer is expressed as $\mu^{\circ}_{aq} - \mu^{\circ}_{ves} = -(RT) \ln K_0$. At 295 °K, this quantity is estimated as −3600 to −3800 cal/mol.

A number of studies (discussed by Tanford, 1973) on the free energy of transfer of aliphatic amphiphiles from water to fluid hydrophobic environments indicate a constant contribution of approximately −700 cal/mol of methylene carbons. In the case of spin-label 1 in equilibrium with PC vesicles lacking a net charge, repulsive contributions to the free energy of transfer are likely to be small, as in the case of nonionic amphiphiles. With this assumption, we estimate that the alkyl chain of spin-label 1 penetrates to the level of the 5th or 6th methylene carbon of the phospholipid fatty acid, consistent with the predictions from space-filling models presented in Figure 4.

Two features, which have facilitated the measurement of surface potentials by distribution techniques and their comparison to theoretical prediction, are the lack of specific interactions between the surface and components of the electrolyte present in the bulk aqueous phase and the response of the nitroxide-labeled probe to surface potential changes in a purely electrostatic manner uncomplicated by specific affinities for negatively-charged phospholipid. A number of studies have indicated that the univalent sodium ions exhibit no specific affinities for the polar moieties of the common phospholipids (Hauser et al., 1975; Inoko et al., 1975; Lis et al., 1975; McLaughlin et al., 1975), and thus a Boltzmann distribution of ions according to thermal equilibrium is a warranted assumption. Absence of specific interactions of spin-label 1 with surface charges is suggested by the demonstration of identical phase distribution ratios for isopotential vesicle preparations containing different concentrations of PA.

We have found that the equilibrium of spin-label 1 in membrane-containing systems reflects the presence of a surface potential having the same dependence on univalent electrolyte concentration, as predicted by the equation of Gouy. In general, the absolute magnitudes of the measured potentials are in reasonable agreement with predicted values, although the potentials obtained by the intensity ratios method (eq 7) are systematically lower for the higher charge densities (4 mol % PA in particular) than expected on the basis of the Gouy equation. This is, perhaps in part, due to approximations involved in spectral analysis, since other methods of extracting data from the spectra (eq 8; double integration) give systematically higher values, although they are more tedious to apply.

Although the Gouy equation rigorously applies only to planar surfaces, its success in accounting for the experimental data presented here on sonicated vesicles is not unexpected. The major difference between the double layer around a spherical particle and a planar surface for charge densities of the magnitude examined here lies in the *spatial dependence* of the potential, and not in the potential *at* the surface (Verwey and Overbeek, 1948). For a sphere of 140 Å radius and an infinite plane of the same charge density, the calculated surface potentials do not differ significantly for most of the charge densities and ionic strengths tested. In fact, in the worst case—very dilute salt (ionic strength ≤0.006) and high charge density (8 mol % PA), the difference is only about 16% in the predicted potential at the surface. For the bulk of our experimental conditions, the difference is ≤5% (Loeb et al., 1961). Thus, we could have applied either the Gouy or the spherical equations for surface potential to generate very similar theoretical curves in Figure 6. Since we are assured that our method estimates potentials *at* the surface only, and is insensitive to the spatial dependence of the double layer, we have chosen to apply the Gouy equation for mathematical simplicity.

In examining the surface charge-dependent differences between potentials derived from our phase distribution data and calculated using the Gouy equation, we did not seek a forced agreement between the two values. Nevertheless, by attending to the discrepancies that do exist, we have brought to mind a number of variables capable of affecting the magnitude of either the measured or the theoretically predicted surface potential (one consideration, involving spectral analysis, has been mentioned above).

(1) Discrepancies observed for vesicles tested at ionic strengths less than 0.01 (most notably in the absence of NaCl, Figure 6) may reflect small errors in estimating the mobile ionic concentration. Furthermore, approximation errors involved in interpreting eq 3 and the use of the Gouy equation are most likely to be significant at very low ionic strength.

(2) Phosphatidic acid, for which the pK of the first acidic dissociation constant is ~3.5 (Abramson et al., 1964), is expected to carry a single negative charge for most of the experimental conditions tested. However, where pH at the vesicle surface is near neutrality (only at very low magnitude surface potentials ($|\psi_0| < 5$ mV)), Abramson et al. (1966) indicate that divalent PA may account for ~10% of the PA population.

By contrast, Johnson (1973) has presented evidence for the significant suppression of ionization of PA in 4 mol % PA–PC sonicated liposomes. If this effect is real, our calculated values of ψ_G would clearly be an overestimate.

(3) ψ_G is calculated based on the underlying assumption that the vesicle surface is smooth with all charged species immobilized in a uniform plane with all other phospholipid head groups. In reality, the vesicle surface is probably quite contoured with charges at different levels within V_{ves}. This evokes uncertainty in the average position of the charge surface. Since the magnitude of the potential declines very steeply with distance in regions of close proximity to the membrane, mea-

surement of surface potentials by phase distribution may deviate from prediction in the direction we observe if the charge surface is not completely accessible to the probe. Thus, the surface representing the average location of membrane-associated spin may be at a lower potential than predicted, resulting in a higher fraction of amphiphile in the aqueous phase.

(4) The calculated magnitudes of ψ_G depend on the choice of σ and the charge density, which in turn depends on the choice of area occupied by each phospholipid molecule in the surface. This represents the only adjustable parameter in our analysis. Physically realistic values for the area per head group in phospholipid bilayers above the thermal transition lie between 60–80 Å^2 (Johnson et al., 1971; Johnson, 1973; Sheetz, 1973). For vesicles, the actual value surely depends on vesicle size and the degree of unsaturation of the phospholipid, but ~70 Å^2/molecule appears to be a reasonable choice. In Figures 6 and 7, we have presented calculated values of ψ_G based on 70 and 80 Å^2/molecule; use of the latter value gives the closest fit of the calculated curve to the data for 4 and 8 mol % PA. There is a reason for considering a value this large for the vesicles of higher charge densities, since we observe that, in our preparations, vesicle size decreases with increasing charge density and smaller vesicles are expected to have a greater area per molecule on the outer surface than larger vesicles.

(5) Changes in the bilayer "fluidity" as a result of composition changes will affect the equilibrium distribution independent of the surface potential. This effect has been minimized by using PA of the same fatty acid composition as the PC and we cannot detect changes in fluidity, as measured by PC spin-labels (Hubbell and McConnell, 1971) over the full composition range of PA–PC used here.

In conclusion, we have demonstrated that a nitroxide-labeled, amphiphilic probe senses the surface potential of phospholipid bilayer vesicles and distributes between the membrane and bulk aqueous phases according to equivalent electrochemical potential. By a series of experimental cross-checks, we have verified that measurements of peak amplitudes taken directly from first derivative spectra can provide a reasonable representation of the nitroxide phase distribution, thus making surface potential estimations by EPR spectroscopy a rapid and simple process.

Although a number of uncertainties in the calculation and interpretation of ψ_G and ψ_s exist, it is clear than predictions of surface potential variations, with charge density and salt concentration based on the Gouy equation, are in tolerable agreement with experimental results. We anticipate its utility as a method for assessing the contribution of surface charge modulation to controlling the interaction of membranes with one another and with other molecules.

Added in Proof

Since submission of this manuscript, a communication has appeared (Gaffney and Mich, 1976) describing a similar estimation of surface potential using paramagnetic amphiphiles on phospholipid liposomes. In agreement with our results, the surface charge densities calculated from phase distribution measurements are compatible with those predicted using the Gouy equation.

Also, an abstract reporting the partition of paramagnetic amphiphiles between biologic membranes and their aqueous surroundings in a manner dependent on electrostatic potential has been presented at the 16th Annual Biophysics Meeting (Melhorn and Packer, 1976).

Appendix

(A) With a representative vesicle diameter of r_0 = 140 Å, a bilayer thickness of 50 Å, and an internal radius of r_i = 90 Å, the total surface area per vesicle is estimated to be $S = 4\pi(r_i^2 + r_0^2) = 3.5 \times 10^5$Å^2. The best value for the molecular area per phospholipid is 70 Å^2, corresponding to 5×10^3 lipids per vesicle. If the phospholipids are distributed according to surface area, there are ~3.5×10^3 lipid molecules on the external surface of the vesicle. At 1, 2, 4, and 8 mol % PA, we expect 35, 70, 140, and 280 molecules of PA on the external surface.

At 1.9% (w/v) lipid in the usual preparation, there are 19 mg of lipid/ml, corresponding to 1.5×10^{19} molecules of lipid (mol wt 765) or 3×10^{15} vesicles. At 2.0×10^{-5} M spin-label 1, there are 1.2×10^{16} label molecules/ml, giving ~4 molecules of label per vesicle.

(B) *Derivation of the Equilibrium Expression (Eq 6).* The volume of the vesicle phase is taken to be proportional to the total mass of the lipid, $V_{ves} = \bar{V}_{ves} m_l$, where $\bar{V}_{ves}$ is the volume of vesicle phase/g of lipid and m_l is the mass of lipid. The volume of the bulk aqueous phase is, of course, proportional to the mass of the bulk aqueous solvent, $V_{aq} = \bar{V}_{aq} m_{aq}$, where $\bar{V}_{aq}$ is the partial specific volume of the solvent and m_{aq} is the mass of the bulk solvent. Thus, eq 4 can be written as

$$\frac{A^-_{f(0)}}{A^-_{b(0)}} = \left(\frac{1}{K\beta}\right)\left(\frac{V_{aq}}{V_{ves}}\right)\left(\frac{m_{aq}}{m_l}\right) \tag{1a}$$

The total mass of solvent in the system, m_T, may be expressed as

$$m_T = m_i + m_{ves} + m_{aq}$$

where m_i, m_{ves}, and m_{aq} are, respectively, the mass of solvent within the vesicle (including hydration of the inner surface), the mass of solvent found in the external vesicle phase, and the mass of solvent in the bulk aqueous phase. The masses m_i and m_{ves} are proportional to the number of vesicles and, hence, to the mass of lipid, $m_i = \bar{m}_i(m_l)$, and $m_{ves} = \bar{m}_{ves}(m_l)$, where $\bar{m}_i$ and $\bar{m}_{ves}$ are the mass of solvent in the vesicle interior and in the vesicle external phase per gram of lipid. Thus,

$$m_{aq} = m_T - m_l(\bar{m}_i + \bar{m}_{ves}) \tag{1b}$$

Therefore, eq 1a becomes:

$$\frac{A^-_{f(0)}}{A^-_{b(0)}} = \left(\frac{1}{K\beta}\right)\left(\frac{V_{aq}}{V_{ves}}\right)\left(\left(\frac{m_T}{m_l}\right) - (\bar{m}_i + \bar{m}_{ves})\right) \tag{1c}$$

By equating $(\bar{m}_i + \bar{m}_{ves})$ with Q, we obtain eq 6 under Results.

(C) *Derivation of Equation for Surface Potentials.* Equation 7 is obtained directly from eq 2, $\psi_s = -(RT/ZF) \ln (K/K_0)$, using the appropriate expressions for K and K_0. From eq 1a,

$$K = \left(\frac{n_b}{n_f}\right)\left(\frac{V_{aq}}{V_{ves}}\right) = \left(\frac{A^-_{b(0)}}{A^-_{f(0)}}\right)\left(\frac{1}{\beta}\right)\left(\frac{m_{aq}\bar{V}_{aq}}{m_l\bar{V}_{ves}}\right)$$

From the definition of α_0 as $K_0\beta(\bar{V}_{ves}/\bar{V}_{aq})$,

$$K_0 = \left(\frac{\alpha_0}{\beta}\right)\left(\frac{\bar{V}_{aq}}{\bar{V}_{ves}}\right)$$

Thus,

$$\psi_s = -\left(\frac{RT}{ZF}\right) \ln \left\{\left(\frac{A^-_{b(0)}}{A^-_{f(0)}}\right)\left(\frac{m_{aq}}{m_l}\right)\left(\frac{1}{\alpha_0}\right)\right\}$$

$$= -\left(\frac{RT}{ZF}\right)\left\{\ln\left(\frac{A^-_{b(0)}}{A^-_{f(0)}}\right) + \ln\left(\frac{m_{aq}}{m_l}\right)\left(\frac{1}{\alpha_0}\right)\right\}$$

which is eq 7.

Equation 8 is obtained in an exactly analogous fashion, using

$$K = \left(\frac{n_b}{n_f}\right)\left(\frac{m_{aq}}{m_l}\right)\left(\frac{\bar{V}_{aq}}{\bar{V}_{ves}}\right)$$

References

Abramson, M. B., Katzman, R., Gregor, H., and Curci, R. (1966), *Biochemistry 5,* 2207–2213.

Abramson, M. B., Katzman, R., Wilson, C. E., and Gregor, H. P. (1964), *J. Biol. Chem. 239,* 4066–4072.

Banks, P. (1966), *Biochem. J. 101,* 18c–20c.

Barton, P. G. (1968), *J. Biol. Chem. 243,* 3884–3890.

Chen, P. S., Toribara, T. Y., and Warner, H. (1956), *Anal. Chem. 28,* 1756–1758.

Davidson, F. M., and Long, D. (1958), *Biochem. J. 69,* 458–466.

Davies, J. T., and Rideal, E. D. (1963), Interfacial Phenomena, New York, N.Y., Academic Press.

Fisher, K. A. (1976), *Proc. Natl. Acad. Sci. U.S.A. 73,* 173–177.

Gaffney, B. J., and Mich, R. J. (1976), *J. Am. Chem. Soc. 98,* 3044–3045.

Hamilton, C. L., and McConnell, H. M. (1968), *Struct. Chem. Mol. Biol.,* 115–149.

Hauser, H., Philips, M. C., Levine, B. A., and Williams, R. J. P. (1975), *Eur. J. Biochem. 58,* 133–144.

Haydon, D. A., and Myers, V. B. (1973), *Biochim. Biophys. Acta 307,* 429–443.

Haydon, D. A., and Seaman, G. V. F. (1967), *Arch. Biochem. Biophys. 122,* 126–136.

Haynes, D. H. (1974), *J. Membr. Biol. 17,* 341–366.

Hubbell, W. L., Metcalfe, J. C., Metcalfe, S. M., and McConnell, H. M. (1970), *Biochim. Biophys. Acta 219,* 415–427.

Hubbell, W. L., and McConnell, H. M. (1971), *J. Am. Chem. Soc. 93,* 314–326.

Inoko, Y., Yamaguchi, T., Furuga, K., and Mitsui, T. (1975), *Biochim. Biophys. Acta 413,* 24–32.

Israelachvili, J. N. (1973), *Biochim. Biophys. Acta 323,* 659–663.

Johnson, S. M. (1973), *Biochim. Biophys. Acta 307,* 27–41.

Johnson, S. M., Bangham, A. D., Korn, E. D. (1971), *Biochim. Biophys. Acta 233,* 820–826.

Kornberg, R. D., and McConnell, H. M. (1971), *Biochemistry 10,* 1111–1120.

Kornberg, R. D., McNamee, M. G., and McConnell, H. M. (1972), *Proc. Natl. Acad. Sci. U.S.A. 69,* 1508–1513.

Kury, P. G., and McConnell, H. M. (1975), *Biochemistry 14,* 2798–2803.

Lis, L. J., Kauffman, J. W., and Shriver, D. H. (1975), *Biochim. Biophys. Acta 406,* 453–464.

Loeb, A. L., Overbeek, J. Th. G., and Wiersema, P. H. (1961), The Electrical Double Layer Around a Spherical Colloid Particle. Cambridge, Mass., The M.I.T. Press, p 30.

McLaughlin, S., Bruder, A., Chen, S., and Moser, C. (1975), *Biochim. Biophys. Acta 394,* 304–313.

McLaughlin, S., and Harary, H. (1976), *Biochemistry 15,* 1941–1948.

McLaughlin, S. G. A., Szabo, G., and Eisenman, G. (1971), *J. Gen. Physiol. 58,* 667–687.

McLaughlin, S. G. A., Szabo, G., Eisenman, G., and Ciani, S. M. (1970), *Proc. Natl. Acad. Sci. U.S.A. 67,* 1268–1275.

Melhorn, R., and Packer, L. (1976), *Biophys. J. 16,* 194a.

Michaelson, D. M., Horwitz, A. F., and Klein, M. P. (1973), *Biochemistry 12,* 2637–2645.

Moller, J. V., and Kragh-Hansen, V. (1975) *Biochemistry 14,* 2317–2323.

Montal, M., and Gitler, C. (1973), *Bioenergetics 4,* 363–382.

Muller, R. U. and Finkelstein, A. (1972a), *J. Gen. Physiol. 60,* 263–284.

Muller, R. U., and Finkelstein, A. (1972b), *J. Gen. Physiol. 60,* 285–306.

Parsegian, V. A. (1969), *Nature (London) 221,* 844–848.

Peifer, J. J. (1962), *Mikrochem. Acta,* 529.

Possmeyer, F., Scherphof, G. L., Dubbelman, T. M. A. R., Van Golde, L. M. G., and Van Deenen, L. L. M. (1969), *Biochim. Biophys. Acta 176,* 95–110.

Romijn, J. C., Van Golde, L. M. G., McElhaney, R. N., and Van Deenen, L. L. M. (1972), *Biochim. Biophys. Acta 280,* 22–32.

Rosenberg, S. A., and Guidotti, G. (1969), *J. Biol. Chem. 244,* 5118–5124.

Rouser, G., Nelson, G. J., Fleischer, S., and Simon, G. (1968), *Biol. Membr., 1968 1,* 5–69.

Seaman, G. V. F., and uhlenbruck, G. (1963), *Arch. Biochem. Biophys. 100,* 493–502.

Sheetz, M. (1973), Ph.D. Thesis, California Institute of Technology.

Singleton, W. S., Gray, M. S., Brown, M. L., and White, J. L. (1965), *J. Am. Oil Chem. Soc. 42,* 53–56.

Stahl, E. (1969), Thin Layer Chromatography, 2nd ed, New York, N.Y., Springer-Verlag.

Tanford, C. (1973), The Hydrophobic Effect, New York, N.Y., Wiley.

Thompson, T. E., and McLees, B. D. (1961), *Biochim. Biophys. Acta 50,* 213–223.

Tinoco, J., Hopkins, S. M., McIntosh, D. J., Sheehan, G., and Lyman, R. L. (1967), *Lipids 2,* 479–483.

Verwey, E. J. W., and Overbeek, J. Th. G. (1948), Theory of the Stability of Lyophobic Colloids, Amsterdam, Elsevier.

Walker, J. A., and Wheeler, K. P. (1975), *Biochim. Biophys. Acta 394,* 135–144.

Yang, S. F., Freer, S., and Benson, A. A. (1967), *J. Biol. Chem. 242,* 477–484.